

Structural and Mechanistic Studies of Polymerase η Bypass of Phenanthriplatin DNA Damage

Mark T. Gregory^{a,c}, Ga Young Park^b, Timothy C. Johnstone^b, Young-Sam Lee^a, Wei Yang^{a,†}, and Stephen J. Lippard^{b,†}

^aLaboratory of Molecular Biology, National Institute of Diabetes and Digestive and Kidney Diseases, National Institutes of Health, Bethesda, MD 20892

^bDepartment of Chemistry, Massachusetts Institute of Technology, Cambridge, MA 02139

^cThe Johns Hopkins University/National Institutes of Health Graduate Partnership Program; National Institutes of Health, Bethesda, MD 20892

Corresponding Author:

Professor Stephen J. Lippard
Department of Chemistry, Room 18-498
Massachusetts Institute of Technology
77 Massachusetts Avenue
Cambridge, MA 02139-4307
lippard@mit.edu
phone: 617-253-1892
fax: 617-258-8150

Short Title:

Polymerase η Bypass of Phenanthriplatin DNA Damage

Contents:

S3-S7 Materials and Methods

S7 References

- S9 **Figure S1.** Evidence of two phenanthriplatin-dG conformations in the insertion complex.
- S9 **Figure S2.** MALDI mass spectra of purified A) 27 mer and B) Pt-27.
- S10 **Figure S3.** MALDI mass spectra of purified A) PPG2, B) Pt-PPG1, C) Pt-PPG2, and D) Pt-PPG3.
- S10 **Figure S4.** Immunoblotting analysis of Pol η expression.
- S11 **Figure S5.** Fidelity of Pol η , Pol ζ , Pol ν , Pol κ , and the Klenow fragment bypassing of phenanthriplatin-damaged DNA at the insertion step.
- S12 **Figure S6.** Model of the Klenow fragment in the insertion step of phenanthriplatin bypass.
- S13 **Figure S7.** Extension complex structure aligned with undamaged structure (4DL3).
- S14 **Table S1:** Macromolecular data collection and refinement statistics
- S15 **Table S2.** Small molecule refinement statistics

Materials and Methods

Materials and Measurements. Cisplatin was obtained from Strem Chemicals, Inc. Oxaliplatin was purchased from LC Laboratories. Phenanthriplatin was synthesized as previously described (1). Oligonucleotides were obtained from Sigma-Aldrich. All other reagents and solvents are commercially available. High-performance liquid chromatography (HPLC) was carried out on an Agilent 1200 series instrument. UV-vis spectroscopy was performed using a HP 8453 UV-visible spectrometer. Atomic absorption spectroscopic measurements were taken on a Perkin Elmer AAnalyst 600 spectrometer. Distilled water was purified by passage through a Millipore Milli-Q Biocel water purification system (18.2 M Ω) equipped with a 0.22 μ m filter. MALDI mass spectrometry was performed at the Koch Institute (MIT) in negative ion mode with an Applied Biosystems model Voyager DE-STR matrix assisted laser desorption ionization (MALDI) time-of-flight mass spectrometer. Electrospray ionization-MS (ESI-MS) data were obtained on an Agilent Technologies 1100 series liquid chromatography/MS instrument. A BioTek Synergy HT multi-detection microplate plate reader was used for MTT and MTS assays.

Oligonucleotide Purification. Four oligonucleotides were purchased from Sigma-Aldrich: Pt-27 (5'-d(CCATCTTACCTCTCCT**G**TACCATCACT)-3'), PPG1 (5'-d(CAT**G**CTCACACT)-3'), PPG2 (5'-d(CAT**G**TCACACT)-3'), and PPG3 (5'-d(CATT**C**GCACACT)-3'). The bolded letters indicate the position of subsequent platination. Oligonucleotides were characterized by HPLC and MALDI (Figures S2 and S3) or ESI-MS. MALDI (margin of error for this method is \pm 8D); 27-mer calculated: 8041.3 Da, found: 8040.773 Da. ESI-MS; PPG1 calculated: 3562.6319 Da, observed: 3564.5 Da; PPG2 calculated: 3562.6319 Da, observed: 3564.6 Da; PPG3 calculated: 3562.6319 Da, observed: 3564.6 Da.

Synthesis of Phenanthriplatin-Modified Pt-27, Pt-PPG1, Pt-PPG2 and Pt-PPG3. A 1.0 mM aqueous solution of phenanthriplatin was combined with 1.2 equiv of silver nitrate in the dark for 5 h to activate the platinum compound. After removal of silver chloride by centrifugation, a portion of the supernatant containing phenanthriplatin was allowed to react with 200.0 nmol of 27-mer, 326.7 nmol of PPG1, 237.1 nmol of PPG2 or 366.8 nmol of PPG3, respectively, in 10 mM NaH₂PO₄ buffer (pH 6.3) in the dark at 37 °C overnight. The platinated Pt-27, Pt-PPG1, Pt-PPG2 and Pt-PPG3 strands were each purified twice or three times by preparative ion-exchange HPLC on a Dionex DNAPac PA-100 column (9x250 mm). After purification, the solutions of platinated DNA were dialyzed against ddH₂O and lyophilized. The final products were stored in ddH₂O at -80 °C. The products were characterized

by ion exchange HPLC, UV-vis spectroscopy, and atomic absorption spectroscopy. Purified Pt-27 (30.27 nmol, 15.0%), Pt-PPG1 (68.58 nmol, 22.4%), Pt-PPG2 (47.34 nmol, 21.8%) and Pt-PPG3 (69.84 nmol, 20.1%) were obtained. The Pt/DNA ratio was determined by AAS and UV-vis spectroscopy to be 0.96 ± 0.04 for Pt-27, 1.10 ± 0.02 for Pt-PPG1, 1.04 ± 0.04 for Pt-PPG2 and 1.08 ± 0.06 for Pt-PPG3. The samples were further analyzed by MALDI mass spectrometry in negative mode. The results are displayed in Figures S2 and S3. Calculated masses for Pt-27, Pt-PPG1, Pt-PPG2 and Pt-PPG3 are 8449.39 Da, 3973.48 Da, 3973.48 Da and 3973.48 Da. The experimentally found masses were 8448.558 Da, 3973.073 Da, 3974.201 Da and 3973.073 Da, respectively.

Cell Lines and Cell Culture. Normal lung fibroblast MRC5 cells were provided by David E. Root (Whitehead Institute for Biomedical Research). The XP30RO cell line (also known as GM3617), which is a SV40 (Simian virus 40)-transformed fibroblast obtained from a patient with XPV (xeroderma pigmentosum variant), was generously offered by Prof. James E. Cleaver at UCSF. GM13154 (XPV, B-Lymphocyte cells) and GM13155 (untransformed XPV fibroblast cells) were purchased from the Coriell Cell Depositories (Coriell Institute, Camden, NJ). Cells were incubated at 37 °C in 5% CO₂ and grown in RPMI (GM13154) or DMEM (MRC5, XP30RO, and GM13155) supplemented with 10% fetal bovine serum and 1% penicillin/streptomycin. Cells were passed every 3 to 4 days and restarted from a frozen stock upon reaching passage number 20.

Immunoblotting Analysis Procedure. Cells (10^6 cells) were scraped into SDS-PAGE loading buffer (64 mM Tris-HCl (pH6.8), 9.6% glycerol, 2% SDS, 5% β-mercaptoethanol, 0.01% Bromophenol Blue) and incubated at 95 °C for 10 min. Whole cell lysates were resolved by 4-20% sodium dodecylsulfate polyacrylamide gel electrophoresis (SDS-PAGE; 200 V for 30 min) followed by electro-transfer to a polyvinylidene difluoride (PVDF) membrane (350 mA for 1 h). Membranes were blocked in 5% (w/v) non-fat milk in PBST (PBS, 0.1% Tween 20) and incubated with the appropriate primary antibody (Anti-DNA polymerase η antibody, Abcam). After incubation with horseradish peroxidase-conjugated secondary antibodies (Goat anti-rabbit), immune complexes were detected with the ECL detection reagent (BioRad) and analyzed using an Alpha Innotech ChemImager™ 5500 fitted with a chemiluminescence filter.

MTT and MTS Assays. The cytotoxicities of cisplatin, oxaliplatin, and phenanthriplatin were evaluated by the MTT (3-(4,5-dimethylthiazol-2-yl)-2,5-diphenyltetrazolium bromide) or MTS (3-(4,5-dimethylthiazol-2-yl)-5-(3-carboxymethoxyphenyl)-2-(4-sulfophenyl)-2H-tetrazolium, inner salt) assay. Solutions of the platinum compounds were freshly prepared in sterile PBS before use and their concentrations were quantitated by atomic absorption spectroscopy. For the MTT assay, cells were

seeded in a 96-well plate (1200 cells per well for XP30RO, and 1800 cells per well for MRC5 and GM13155) in 100 μ L of DMEM and incubated for 24 h. The cells were treated with cisplatin, oxaliplatin, or phenanthriplatin, separately at varying concentrations, for an incubation period of 72 h at 37 °C. The cells were then treated with 20 μ L of MTT (5 mg/mL in PBS) and incubated for 4 h. The medium was removed, 100 μ L of DMSO was added to the cells, and the absorbance of the purple formazan dye was recorded at 570 nm using a BioTek Synergy HT multi-detection microplate plate reader. For each cell line, three independent experiments were carried out in triplicate. For MTS assay, GM13154 cells were seeded in a 96-well plate (50000 cells per well) in 50 μ L of RPMI and were then treated with cisplatin, oxaliplatin, or phenanthriplatin, separately at varying concentrations, for an incubation period of 72 h at 37 °C. The cells were then treated with 20 μ L of MTS/PMS solution, 20:1 = MTS (2 mg/mL in PBS): PMS (phenazine methosulfate, 0.92mg/ml in PBS), and incubated for 4 h at 37 °C. To measure the amount of soluble formazan produced by cellular reduction of the MTS, the absorbance at 490 nm was measured.

Small Molecule X-ray Crystallography. Crystals of *cis*-diammine(phenanthridine)(9-ethylguanine) trifluoromethanesulfonate, prepared as previously described (2), were grown at room temperature by slow evaporation of an aqueous solution of the compound. The solution was not allowed to evaporate completely and the crystals were preserved in the mother liquor. The compound crystallized as well-faceted colorless blocks. A sample suitable for X-ray diffraction was selected under crossed-polarizers, mounted on a nylon cryoloop in Paratone oil, and cooled to 100 K under a stream of nitrogen. A Bruker APEX CCD X-ray diffractometer controlled by the *APEX2* software was used to record the diffraction of graphite-monochromated Mo K α radiation ($\lambda = 0.71073 \text{ \AA}$) (3). Although the crystals were of high quality, the resolution was limited. As described below, this feature most likely arises from significant disorder of within one of the crystallographically independent molecules in the asymmetric unit. The data were integrated with *SAINT* (4) and absorption, Lorentz, and polarization corrections were calculated with *SADABS* (5). The space group was determined by analyzing the Laue symmetry and the systematically absent reflections with *XPREP* (6). The structure was solved using direct methods and refinement was performed with the *SHELX-97* program suite (7, 8). Refinement was carried out against F^2 using standard procedures (9). Non-hydrogen atoms within the platinum complexes were located in difference Fourier maps during refinement. The limited resolution only permitted anisotropic refinement of the non-carbon atoms. Counter ions and solvent molecules could not be located in the difference Fourier maps. Hydrogen atoms were not included in the final model. The rings of the phenanthridine ligands were constrained to hexagonal-planar geometry. No higher

symmetry or twinning was detected with *PLATON* (10, 11). Final refinement details are presented in Table S2. The structure was deposited in the Cambridge Structural Database (CCDC 993359),

Run off polymerization assay. Pol η 1-432aa was cloned, expressed, and purified as described previously (12). Pol ν and Pol ζ were cloned, expressed, and purified as described previously (13). Klenow fragment was obtained from New England Biolabs (Pdt# M0210S). Pol κ was obtained from Enzymax (cat# 27).

The template/primer pairs used are shown in Figure 1B and 1C. The reaction mixture contained 0-50nM Polymerase, 25 mM each dNTP, 100 nM 5' labeled primer and template, 40 mM Tris pH 7.5, 5 mM MgCl₂, 100 mM KCl, 10 mM dithiothreitol, 0.1mg/ml bovine serum albumin, and 5% glycerol. Reactions were initiated by addition of dNTP and MgCl₂, incubated at 30 °C for 5 min (10 min for Pol ζ), and quenched with an equal volume of formamide, 10 mM NaOH, and xylene cyanol. After heating at 90 °C for 3 min and rapid cooling on ice, the primers were resolved on 20% polyacrylamide (15% for Pol ζ) gels containing 5.5 M urea, visualized using a Typhoon Trio (GE Healthcare), quantified using ImageQuantTL (GE Healthcare) software.

Nucleotide preference assay. Nucleotide preference was measured using the template/primer pairs shown in Figure 1D. The reaction mixture contained 2 nM Pol η , 25 mM dNTP, 5 mM 5' labeled primer and template, 40 mM Tris pH 7.5, 5 mM MgCl₂, 100 mM KCl, 10 mM dithiothreitol, 0.1 mg/ml bovine serum albumin, and 5% glycerol. Reactions were initiated by addition of dNTP and MgCl₂, incubated at room temperature for 5 min, and quenched with an equal volume of formamide, 10 mM NaOH, and xylene cyanol. After heating at 90 °C for 3 min and rapid cooling on ice the primers were resolved on 20% polyacrylamide gels containing 5.5 M urea and visualized using a Typhoon Trio (GE Healthcare), quantified using ImageQuantTL (GE Healthcare) software.

Steady-state kinetic assay. Steady-state kinetic parameters K_M and K_{cat} were measured using the template/primer pairs shown in Figure 1D. The reaction mixture contained 2.5 or 5 nM Pol η , 0-60 mM dNTP, 5 mM 5' labeled primer and template, 40 mM Tris pH 7.5, 5 mM MgCl₂, 100 mM KCl, 10 mM dithiothreitol, 0.1 mg/ml bovine serum albumin, and 5% glycerol. Reactions were initiated by addition of dNTP and MgCl₂, incubated at room temperature for 5 min, and quenched with an equal volume of formamide, 10 mM NaOH, and xylene cyanol. After heating at 90 °C for 3 min and rapid cooling on ice, the primers were resolved on 20% polyacrylamide gels containing 5.5M urea, visualized using a Typhoon Trio (GE Healthcare), and quantified using ImageQuantTL (GE Healthcare) software. Curve fitting was performed using Prism 5 (Graphpad) software.

Macromolecular Crystallization and Data Collection. For crystallization, purified Pol η was mixed in a 1:1.09 ratio with DNA in 5 mM MgCl₂ and incubated to form a binary complex. DNA of the sequence 5'-CATGCTCACACT -3' (phenanthriplatin damaged G is underlined) and 5'-AGTGTGAG -3' were used to form the insertion step complex. DNA of sequence 5'-CATCGTCACACT -3' (phenanthriplatin damaged G is underlined) and 5'-AGTGTGAG -3' were used to form the extension step complex. After threefold dilution to reduce salt concentration to 150 mM KCl, the solution was concentrated to 3.5 mg/ml and the correct dNMPNPP was added to form the ternary complex. Crystals were obtained using the hanging drop method over a reservoir containing 0.1M MES pH 6.0, 15% (insertions step crystal) or 22% (extension step crystal) PEG 2000MME. After a short soak in 0.1 M MES pH 6.0, 20% PEG 2000MME, and 20% glycerol for cryoprotection, the crystals were flash frozen in liquid nitrogen. Diffraction data were collected at 100 K on the 22 BM beam line at the Advanced Photon Source (APS).

Macromolecular Structural Determination. Diffraction data were processed with HKL2000 and converted to structure factors by TRUNCATE (14-16). Both data sets were in the P6₁ space group and isomorphous with the Pol η structure with undamaged DNA substrate (PDB code 3MR2), which was used to obtain phases. Models were built in COOT and refined in PHENIX (17, 18). Data collection and refinement statistics are summarized in supplemental table S1. All structural figures were rendered in PyMol (19).

References

1. Park GY, Wilson JJ, Song Y, Lippard SJ (2012) Phenanthriplatin, a monofunctional DNA-binding platinum anticancer drug candidate with unusual potency and cellular activity profile. *Proc Natl Acad Sci USA* 109(30):11987-11992.
2. Johnstone TC, Lippard SJ (2014) The chiral potential of phenanthriplatin and its influence on guanine binding. *J Am Chem Soc*:DOI: 10.1021/ja4125115.
3. Anonymous (2008) APEX2 (Bruker AXS, Inc, Madison, WI), 2008-4.0.
4. Anonymous (2008) SAINT: SAX Area-Detector Integration Program (University of Göttingen, Göttingen, Germany), 2008/1.
5. Sheldrick GM (2008) SADABS: Area-Detector Absorption Correction (University of Göttingen, Göttingen, Germany).
6. Anonymous (2008) XPREP (Bruker AXS, Madison, WI), 2008/2.
7. Sheldrick GM (2000) SHELXTL-97 (University of Göttingen, Göttingen, Germany).
8. Sheldrick GM (2008) A short history of SHELX. *Acta Crystallogr Sect A* 64:112-122.
9. Müller P (2009) Practical suggestions for better crystal structures. *Crystallogr Rev* 15(1):57-83.
10. Spek AL (2003) Single-crystal structure validation with the program PLATON. *J Appl Crystallogr* 36:7-13.
11. Spek AL (2008) PLATON, A Multipurpose Crystallographic Tool (Utrecht University, Utrecht, The Netherlands).
12. Biertümpfel C, et al. (2010) Structure and mechanism of human DNA polymerase η . *Nature* 465(7301):1044-U1102.

13. Lee Y-S, Gregory MT, Yang W (2014) Human Pol ζ purified with accessory subunits is active in translesion DNA synthesis and complements Pol η in cisplatin bypass. *Proc Natl Acad Sci USA* DOI: 10.1073/pnas.1324001111.
14. French S, Wilson K (1978) On the treatment of negative intensity observations. *Acta Crystallogr A* 34(4):517-525.
15. Otwinowski Z, Minor W (1997) Processing of X-ray diffraction data collected in oscillation mode. *Method Enzymol* 276:307-326.
16. Winn MD, et al. (2011) Overview of the CCP4 suite and current developments. *Acta Crystallogr D* 67:235-242.
17. Adams PD, et al. (2010) PHENIX: a comprehensive Python-based system for macromolecular structure solution. *Acta Crystallogr D* 66:213-221.
18. Emsley P, Lohkamp B, Scott WG, Cowtan K (2010) Features and development of Coot. *Acta Crystallogr D* 66:486-501.
19. Schrodinger L (2010) The PyMOL Molecular Graphics System, Version 1.3r1.

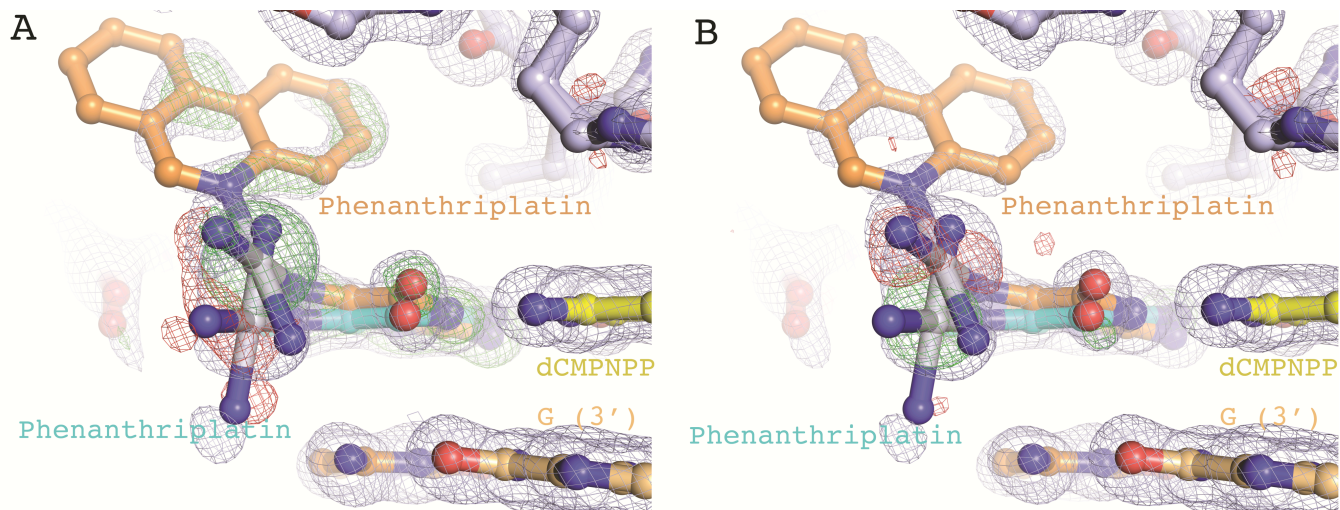


Figure S1. Evidence of two phenanthriplatin-dG conformations in the insertion complex.

A. Insertion complex phenanthriplatin-dG masked by $2F_o - F_c$ (blue) and $F_o - F_c$ (green/red) maps calculated having omitted the major conformation.

B. Insertion complex phenanthriplatin-dG masked with $2F_o - F_c$ (blue) and $F_o - F_c$ (green/red) maps calculated having omitted the minor conformation.

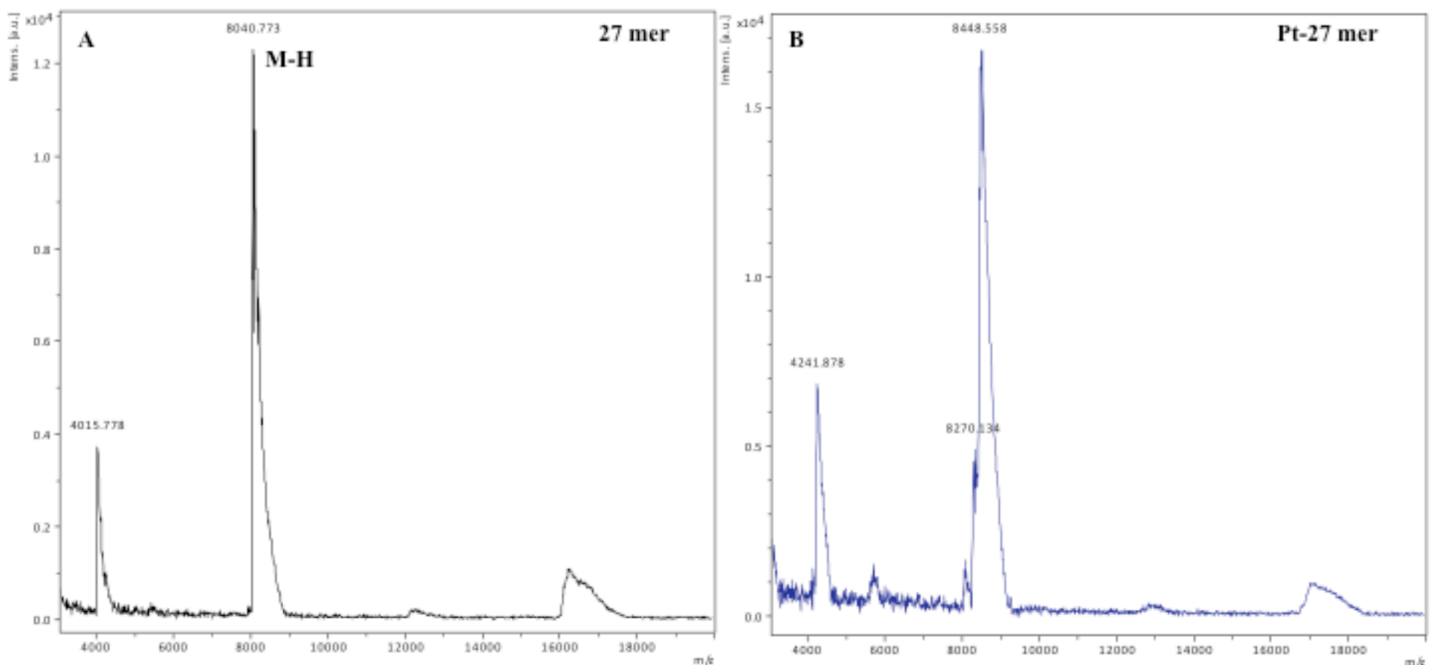


Figure S2. MALDI mass spectra of purified A) 27 mer and B) Pt-27.

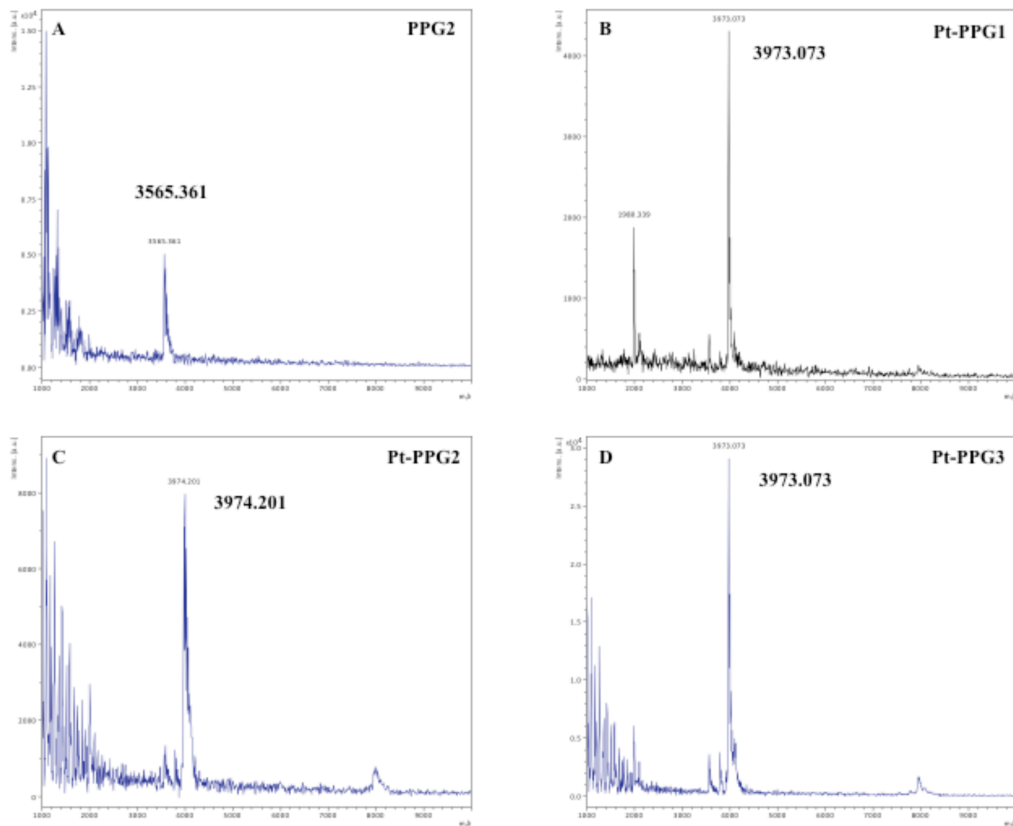


Figure S3. MALDI mass spectra of purified A) PPG2, B) Pt-PPG1, C) Pt-PPG2, and D) Pt-PPG3.

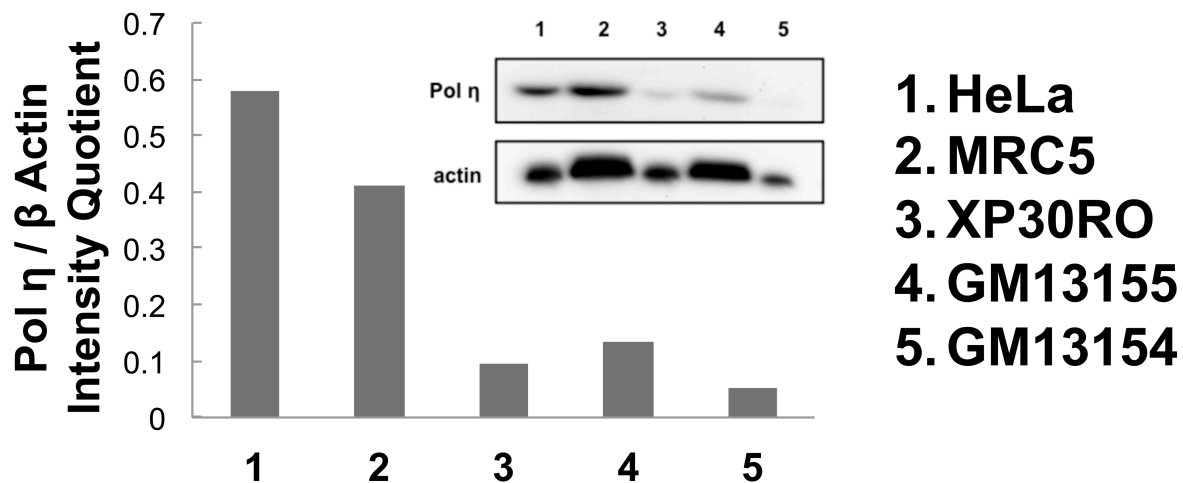


Figure S4. Immunoblotting analysis of Pol η expression in XPV cell lines (XP30RO, GM13155, and GM13154), MRC5, and HeLa cells. Whole cell lysates were resolved by SDS-PAGE and analyzed by immunoblotting against pol η and β -actin (loading control). Histogram depicts the quotient of the integrated areas of the Pol η and β actin bands for each sample. Inset is the image of the blotted film.

3' TCACTACCATGTCCTCTCCATTCTACC
5' AGTGATGGTA

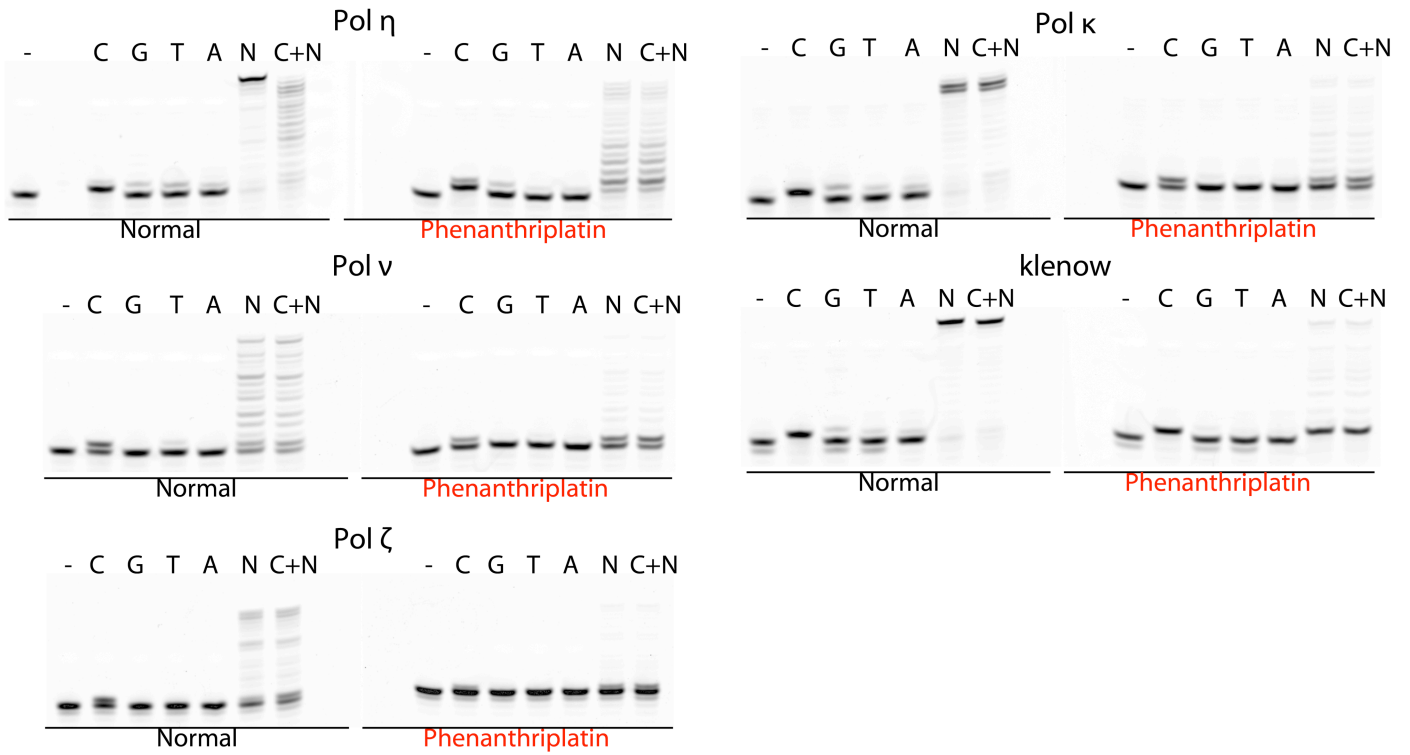


Figure S5. Fidelity of Pol η , Pol ζ , Pol v , Pol κ , and the Klenow fragment bypassing of phenanthriplatin-damaged DNA at the insertion step.

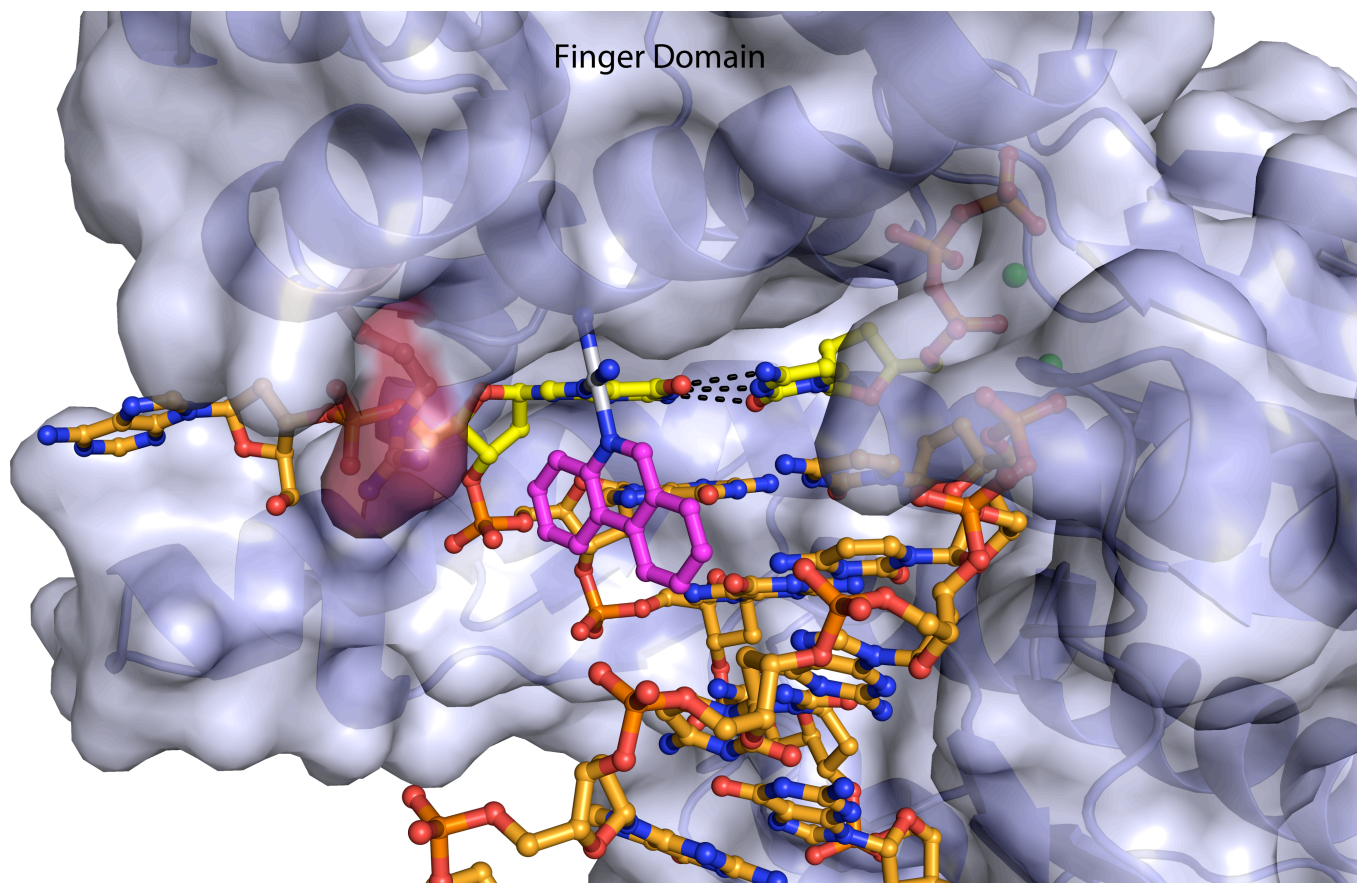


Figure S6. Model of the Klenow fragment in the insertion step of phenanthriplatin bypass. The phenanthriplatin adduct is rotated $\sim 180^\circ$ from the observed position in the Pol η structures due to lack of a pocket in the finger domain. An arginine residue had to be moved to a different rotamer position in order to fit the adduct and is highlighted in red in the surface representation.

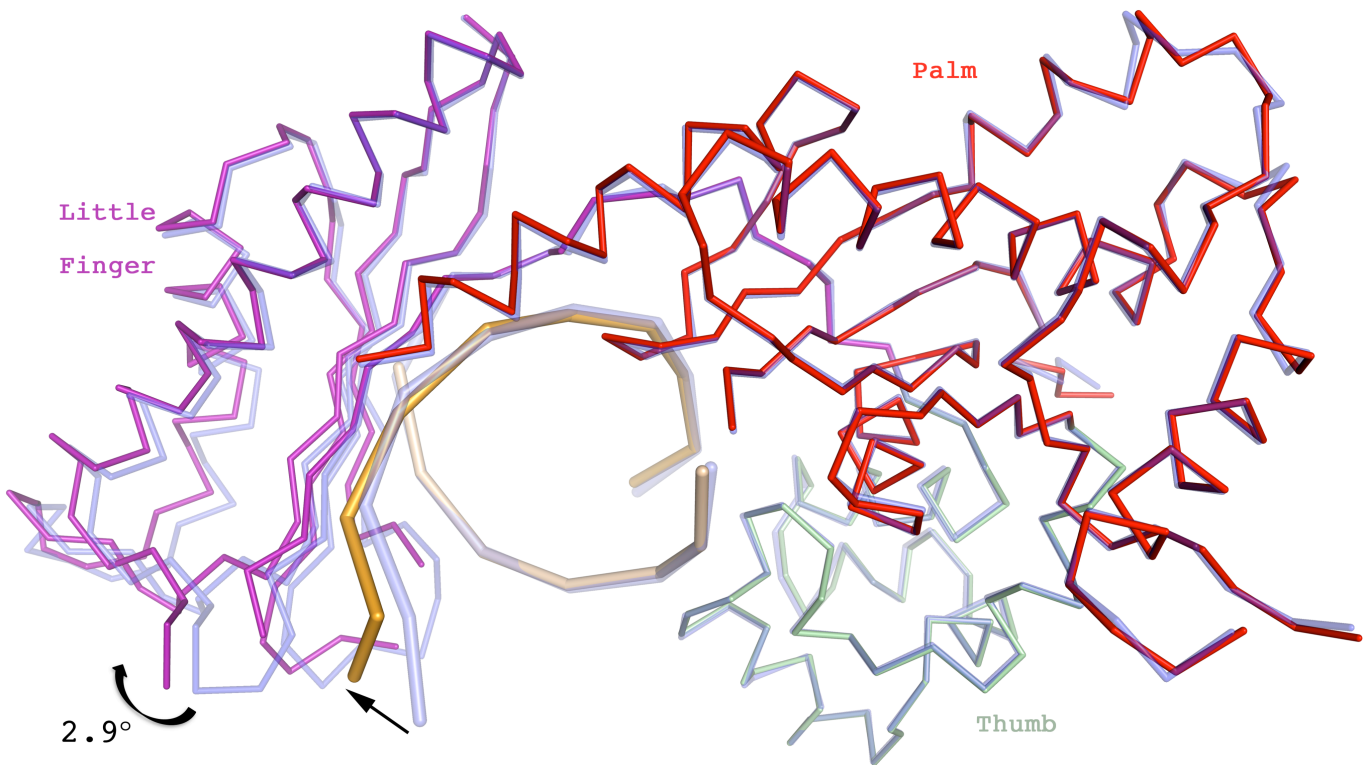


Figure S7. Extension complex structure aligned with undamaged structure (4DL3). The extension complex is colored by domain and the undamaged structure is semitransparent blue. The shift in DNA position downstream of the adduct is shown with a straight arrow and the rotation of the little finger domain is denoted with curved arrow. The finger domain is omitted for clarity.

Table S1: Macromolecular data collection and refinement statistics

	Insertion	+1 Extension
PDB code	4Q8E	4Q8F
Data Collection		
Space group	<i>P</i> 6 ₁	<i>P</i> 6 ₁
Cell dimensions		
<i>a</i> , <i>b</i> , <i>c</i> (Å)	98.77	98.69
	98.77	98.69
	82.20	81.81
Wavelength (Å)	1.00	1.00
Resolution (Å)	30-1.55	30-2.80
Rsym (%) [*]	7.8 (66.0)	8.9 (55.9)
<i>I</i> / σ [*]	8.15 (2.16)	12.58 (1.78)
Completeness (%) [*]	99.7 (98.6)	99.6 (97.52)
Redundancy [*]	3.4 (3.2)	3.5 (2.9)
Refinement		
Resolution (Å)	30-1.55	30-2.80
No. reflections	65924	11236
<i>R</i> _{work} / <i>R</i> _{free}	18.3/22.5	19.6/24.3
No. atoms		
Protein/DNA	3464/426	3258/497
dNMPNPP/Mg ²⁺	28/2	62/2
Water/Solutes	394/18	39/30
B-factors		
Protein/DNA	21.24/23.29	35.47/40.54
dNMPNPP/Mg ²⁺	9.64/7.30	25.26/22.82
Water/Solutes	26.80/24.55	26.32/36.82
R.m.s deviations		
Bond lengths (Å)	0.01	0.003
Bond angles (°)	1.4	0.84

^{*} Highest resolution shell is shown in parenthesis

Table S2. Small molecule refinement statistics

Formula	C ₂₀ H ₂₃ N ₈ OPt
Space group	$\bar{P}1$
<i>a</i> , Å	13.0839(12)
<i>b</i> , Å	13.3405(12)
<i>c</i> , Å	16.8639(16)
α, °	98.744(2)
β, °	93.9530(10)
γ, °	93.505(2)
<i>V</i> , Å ³	2894.7(5)
<i>Z</i>	4
<i>T</i> , K	100(2)
μ(Mo Kα), mm ⁻¹	4.869
θ range, °	1.55 to 22.49
total no. of data	35898
no. of unique data	7475
no. of parameters	611
completeness (%)	98.6
R ₁ ^a (%)	4.74
wR ₂ ^b (%)	13.76
GOF ^c	1.084

^aR₁ = $\frac{\sum ||F_o| - |F_c||}{\sum |F_o|}$. ^bwR₂ = $\{\frac{\sum [w(F_o^2 - F_c^2)^2]}{\sum [w(F_o^2)^2]}\}^{1/2}$.

^cGOF = $\{\frac{\sum [w(F_o^2 - F_c^2)^2]}{(n-p)}\}^{1/2}$